Molecular Neurobiology (2025) 62:6983–6997
https://doi.org/10.1007/s12035-024-04629-z

RESEARCH

NEFL Modulates NRN1-Mediated Mitochondrial Pathway to Promote Diacetylmorphine-Induced Neuronal Apoptosis

Sensen Zhu[1] · Liping Su[3] · Mengjie Zhuang[1] · Li Liu[3] · Min Ji[3] · Jingyu Liu[1] · Chenlu Dai[1] · Jinling Xiao[1] · Yaling Guan[1] · Long Yang[5] · Hongwei Pu[1,2,4]

Received: 20 May 2024 / Accepted: 12 November 2024 / Published online: 19 November 2024

Abstract

Diacetylmorphine abuse is a major social problem that jeopardizes the world, and abuse can cause serious neurological disorders. Apoptosis plays an important role in neurological diseases. A previous study by our group found that the brain tissue of diacetylmorphine-addicted rats showed severe vacuole-like degeneration and increased apoptosis, but the exact mechanism has not yet been reported. We used TMT technology to sequence the diseased brain tissue of rats, and selected neurofilament light chain (NEFL) and neuritin (NRN1) as the focus of our research. We explore the possible roles and mechanisms played by both. Based on the construction of apoptotic cell model, we used overexpression/silencing lentiviral vectors to interfere with the expression of NEFL in PC12 cells, and the results suggested that NEFL could regulate NRN1 to affect the apoptosis level. To further understand the specific mechanism, we used transmission electron microscopy to observe the ultrastructure of apoptotic cells, and the results showed that compared with the control group, mitochondria in the model group showed obvious vacuolation as well as expansion, a significant increase in the accumulation of ROS, and a significant decrease in the mitochondrial membrane potential; after overexpression/silencing of NEFL, these changes were found to occur along with the alteration of NEFL expression. In summary, we conclude that diacetylmorphine induces neuronal apoptosis, and the specific mechanism is that NEFL regulates the NRN1-mediated mitochondrial pathway to promote apoptosis.

Keywords Diacetylmorphine · Neuronal apoptosis · Mitochondrial pathway · NEFL · NRN1

Introduction

Diacetylmorphine, as an opioid, is abused due to its strong euphoric effects [1]. The World Drug Report 2023 shows that 60 million people are predicted to be using opioids in 2021, of which nearly 52.5%, or 31.5 million, have heroin use. It is worth noting that opioids remain the deadliest class of drugs, with directly related deaths accounting for approximately 2/3 of all drug deaths each year, and the majority of deaths are due to abuse [2]. It has been suggested that diacetylmorphine can cause severe neurological damage and induce a variety of neurological disorders [3, 4]. Therefore, it is of great significance to investigate the mechanism of neurological damage caused by diacetylmorphine to provide a solid theoretical basis for the clinical treatment of "chasing the dragon" patients.

The phenomenon of apoptosis was discovered in 1965 as a form of programmed cell death [5]. In ischemic stroke research, Li team [6] found that, dong quai methylin can alleviate the abnormal apoptosis level of neurons, and the

Sensen Zhu, Liping Su, and Mengjie Zhuang are co-first authors of the article.

✉ Long Yang
1449071175@qq.com

✉ Hongwei Pu
576250630@qq.com

1 School of Basic Medical Science, Xinjiang Medical University, Urumqi 830017, China

2 Key Laboratory of Forensic Medicine, Xinjiang Medical University, Xinjiang, China

3 Department of Pathology, The First Affiliated Hospital of Xinjiang Medical University, Xinjiang, China

4 Department of Discipline Construction, The First Affiliated Hospital of Xinjiang Medical University, Urumqi 830054, China

5 Department of Anesthesiology, The First People's Hospital of Foshan, Foshan City 528000, China

mitochondrial pathway plays an indispensable role in it. Some scholars found that, in traumatic brain injury, neuronal cells showed severe mitochondrial dysfunction, which in turn led to the occurrence of apoptosis, and the specific mechanism was the elevation of ROS and calcium ion levels [7].

NEFL, as a neurofilament light chain protein, has the functions of maintaining neuronal skeleton structure, axon caliber, and regulating programmed death, and plays an important role in a variety of diseases. Li, in a study on AD, found that NEFL was a hub gene closely related to oxidative stress when analyzing the relevant data sets in GEO using raw letter technology, and the specific mechanism was not explored in depth [8]. In head and neck cancers, NEFL induces apoptosis and inhibits invasion [9]. However, studies on whether NEFL regulates neuronal apoptosis are still rarely reported, and related studies are urgently needed to be supplemented.

NRN1 is a small, highly conserved extracellular membrane protein that exerts neurotrophic effects and promotes neuronal synapse growth, and was first identified by Nedivi in 1993 [10]. NRN1 is expressed in late mitotic differentiated neurons and neuronal structures associated with plasticity in the nervous system, and is regulated by neural activity and neurotrophic factors. In studies related to schizophrenia (SZ), the expression level of NRN1 is closely related to brain activity in SZ patients, and can be used as a potential target gene [11]. In studies of esophageal cancer, NRN1 inhibits the PI3K-Akt-mTOR pathway on the invasion and migration of esophageal cancer cells [12]. In a rat optic nerve crush injury model, NRN1 activates the AKT and STAT3 pathways and is closely involved in the mitochondrial apoptosis pathway, and overexpression of NRN1 effectively reduces retinal ganglion cell apoptosis and improves optic nerve function in rats [13].

Mitochondria, as energy processing plants of cells, are involved in multiple metabolic pathways and various biological processes, for example, apoptosis of the mitochondrial pathway [14].Accumulation of ROS, disruption of mitochondrial morphology, and decrease in membrane potential are typical manifestations of mitochondrial apoptosis [15].While studying possible therapeutic regimens for neuroblastoma (NB), Kommalapati found that chloroquine (CQ)-induced autophagy inhibition phenomenon would reduce the mitochondrial membrane potential (MMP) and ultimately lead to apoptosis in NB cells [16]. In the study of circadian regulation of liver function, interference with Clock expression will restore mitochondrial membrane potential and inhibit the mitochondrial apoptotic pathway by suppressing the increase in mitochondrial membrane permeability, reducing hepatocyte injury [17]. It is worth noting that mitochondrial apoptosis is one of the major apoptotic pathways.

In the current study, we found that diacetylmorphine will cause a significant increase in neuronal apoptosis levels. To understand the specific mechanisms, we explored the role of NEFL and NRN1 in diacetylmorphine-induced neuronal apoptosis. Interference with NEFL expression was found to affect NRN1 expression and apoptosis levels in the model, and NEFL-induced apoptosis by regulating the NRN1-mediated mitochondrial pathway. Our study further clarifies the possible mechanisms of neuronal apoptosis caused by diacetylmorphine, provides a theoretical basis for the clinical treatment of brain injury in diacetylmorphine-addicted patients, and complements research in related fields.

Methods and Materials

Reagents

Hematoxylin–eosin (HE) stain kit (G1120, Beijing Solarbio Science & Technology Co., Ltd.), Hoechst 33342/PI Double Stain Kit (CA1120, Beijing Solarbio Science & Technology Co., Ltd.), Reactive Oxygen Species Assay Kit (CA1410, Beijing Solarbio Science & Technology Co.,Ltd), Mitochondrial Membrane Potential Assay Kit with JC-1 (M8650, Beijing Solarbio Science & Technology Co., Ltd), BCA Protein Assay Kit (PC0020, Beijing Solarbio Science & Technology Co., Ltd.), SDS-PAGE Gel Kit (P1200, Beijing Solarbio Science & Technology Co., Ltd.), Nissl staining solutio (G1036, servicebio), In Situ Cell Death Detection Kit, TMR red (12156792910, Roche), CCK-8 (PF0004, Proteintech Group, Inc.), recombinant proteinase K (G1234, servicebio) PE Annexin V Apoptosis Detection Kit I (559763, Becton Dickinson and Company), ultra-ultrasensitive ECL chemiluminescent substrate (BL520A, Biosharp). Sources of all the primary antibodies used in the study are listed in Table 1. All secondary antibodies conjugated with horseradish peroxidase were from Proteintech Group, Inc.

In Vivo Experiments

Zoomorphosis

In this study, the diacetylmorphine-induced rat addiction model was constructed on the basis of the group's previous research [18], and the specific operation was as follows: 8-week-old male SD rats with an initial body weight of 210 ± 10 g were selected, and divided into the normal group and the diacetylmorphine group. The normal group was injected with saline subcutaneously, and the diacetylmorphine group was injected with diacetylmorphine subcutaneously (the amount of drug injected subcutaneously was 5 mg/kg on the first day, and then the amount of drug injected was increased by 2 mg/kg per day, and it was once a day at 10:00 and 19:00), and the rats were subjected to naloxone hydrochloride hyperexpression test on the 20th

Table 1 Details of the primary antibodies used in the study

Antibody	Full name of indicator	Cat	WB dilution	Source
Mouse monoclonal antibody [DA2] to 68 kDa neurofilament/NF-L	Neurofilament light chain	ab7255	1:5000	Abcam plc
Neuritin (B-9)	Neuritin	sc-365538	1:2000	Santa Cruz Biotechnology
Rabbit polyclonal antibody to Bax	BCL2-associated X	ab7977	1:2000	Abcam plc
Bcl-2 rabbit mAb	B cell lymphoma-2	A19693	1:2000	ABclonal Biotechnology Co., Ltd
Caspase-3 rabbit pAb	Caspase-3	A0214	1:1000	ABclonal Biotechnology Co., Ltd
Rabbit monoclonal antibody [E23] to caspase-9	Caspase-9	ab32539	1:1000	Abcam plc
Cytochrome c antibody	Cytochrome c oxidase	4272	1:2000	Cell Signaling Technology
Mouse monoclonal antibody [N152B/23] to VDAC1/Porin	Voltage-dependent anion channel 1	ab186321	1:2000	Abcam plc
β-Tubulin antibody	Tubulin beta class I	2146	1:2000	Cell Signaling Technology

day, each rat was observed for 30 min, with specific observations of body twisting, wet dog-like shaking, jumping, and tooth chattering. And the rat was executed using the method of cervical vertebral dislocation after complying with the requirements. All experimental rats were kept in individually ventilated cages with free access to food and water. All animal experiments were conducted in accordance with ARRIVE guidelines. All methods were performed in accordance with relevant guidelines and regulations.

Hematoxylin–Eosin Stain

Take paraffin section of rat brain tissue from Control group and Model group, bake the slices in oven at 65 °C for 1h, deparaffinize the slices in xylene I/II for 15 min, gradient ethanol to water for 5 min in each group, hematoxylin was applied to the slides in a volume of 200 μl/sheet. Let it stand for 3 min, wash away the excess staining solution in water, and observe the staining under the microscope, the nucleus was blue-purple, and the cytoplasm was basically colorless. Eosin was applied in a volume of 200 μl/sheet to the slide just above, left for 5 min, washed away the excess staining solution, and the staining was observed under the microscope, and the cytoplasm was red or pink. The cytoplasm was red or pink. The slides were dehydrated with anhydrous ethanol for 1 min and sealed with neutral resin.

Nissl Staining

Take paraffin section of rat brain tissue from control group and model group, refer to the same method of dewaxing and to water as above, and prepare the working solution for Nissl staining, cover slides with 200 μl of staining solution each, let it stand for 3 min at room temperature, and wash it with water until the water stream is colorless. Under the microscope, the Nissl body was dark blue, and the background was light blue or colorless. After baking and drying, neutral resin was used to seal the sections.

Hoechst33342

Animal experiments: take paraffin sections of brain tissue of the same grouping as above and carry out the same method of dewaxing as above, to water. Configure the Hoechst33342 staining working solution by quantizing 5 μl of Hoechst33342 stain stock solution to 1 ml using the staining buffer in the kit. Use the Hoechst33342 staining working solution prepared in advance to spread evenly on the sections, avoid light and room temperature fixation for 15 min, and then, use distilled water to clean it three times, each time for 5 min. Use an anti-fluorescence quencher to seal the film. Cellular experiments: in six-well plate spread in advance to 5×105 cells/well, in different interventions After the end, PBS was washed three times, 4% paraformaldehyde was fixed for 30 min at room temperature, PBS was washed three times, 5 min each time, 1 ml of Hoechst33342 staining working solution was added to each well, protected from light, and stood at room temperature for 15 min. PBS was washed three times, 5 min each time. Cells emitting bright blue fluorescence were judged as apoptotic cells under fluorescence inverted microscope for observation.

Tunel Staining

Take paraffin section of rat brain tissue from control group and model group, and dewax the paraffin sections according to the above method, to water, according to the reagent instructions; the configured recombinant proteinase K working solution was spread on the sections, incubated at room temperature for 30 min, and washed off and then configuration of Tunel's reaction solution (blue:red = 1:9). And cover the slides with the staining solution in a volume of 50 μl per slide and incubate at 37 °C, protected from light, for 60 min. Excess stain was washed away, and the film was blocked with a putative fluorescence quencher and then observed under a fluorescence microscope; the cells emitting red fluorescence were determined as apoptotic cells.

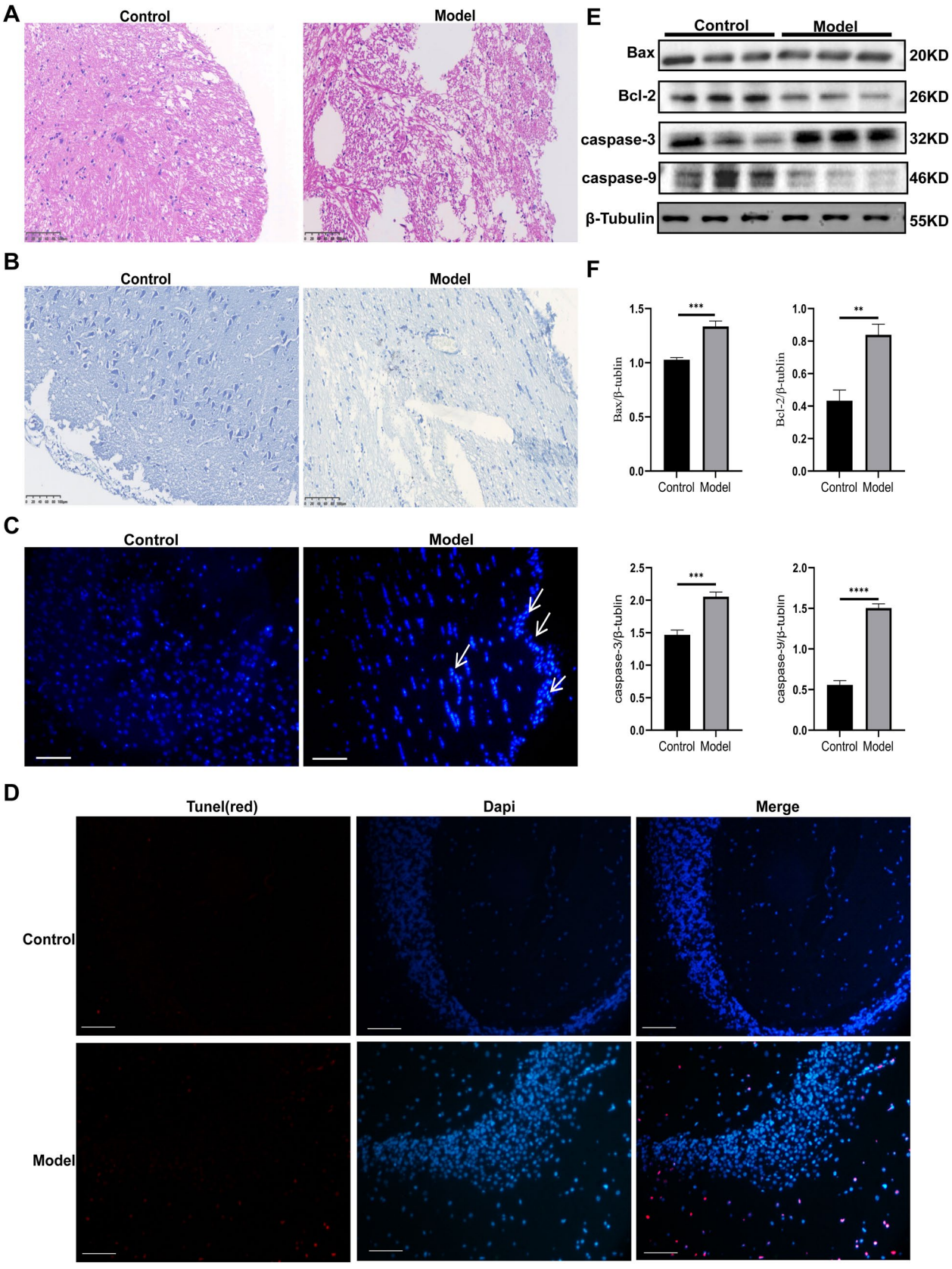
A
Control
Model
B
Control
Model
C
Control
Model
D
Tunel(red)
Dapi
Merge
Control
Model
E
Control
Model
Bax
Bcl-2
caspase-3
caspase-9
β-Tubulin
20KD
26KD
32KD
46KD
55KD
F
Bax/β-tublin
Bcl-2/β-tublin
caspase-3/β-tublin
caspase-9/β-tublin
Control
Model

◂**Fig. 1** Increased apoptosis in brain tissues of addicted SD rats. **A** Representative images of HE staining of brain tissue injury sites in addicted rats, scale bar 100 μm; **B** Representative images of Nissl staining of brain tissue injury sites in addicted rats, scale bar 100 μm; **C**, **D** Fluorescent staining of apoptotic cells Hoechst33342 in brain tissue injury sites in addicted rats, scale bar 100 μm; **E** Western blot for caspase-3, caspase-9, Bax, and Bcl-2 protein expression levels; **F** statistics of E, compared with control, $*P<0.1$, $**P<0.01$, $***P<0.001$

Western Blot

Total protein extracts of brain tissue/intracellular/mitochondrial at the site of injury were used using RIPA buffer (Solarbio) containing 1% protease inhibitor, phosphatase inhibitor and PMSF. Determination of protein concentration was performed using the BCA Protein Quantification Kit (Solarbio). Proteins were separated using SDS-PAGE (Solarbio) and pre-stained protein molecular weight standard maker (epizyme) for protein molecular weight estimation. Transblots were performed using 0.45-μm PVDF membranes (Millipore), incubated for 2 h at room temperature with 5% skimmed milk for closure, and washed three times for 5 min each with TBST (servicebio) before placing the membranes in primary antibody buffer and incubating them at 4 °C overnight. The following day, at room temperature, the membranes were closed for 1.5 h using mouse/rabbit secondary antibody (1:2000, Proteintech). PVDF membranes were developed using the ECL kit (Biosharp).

Bioinformatics Analysis

TMT proteomics sequencing using tissues from brain injury sites of diacetylmorphine-addicted rats (Novogene) and visualization of heatmaps and volcano plots of significantly differentially expressed genes using the R language and (GO) functional annotation and Kyoto Encyclopedia of Genes and Genomes (KEGG) pathway analysis. The version of R used for the analysis was R4.4.0 [19], and the R packages used were dplyr [20], tidyverse [21], ggplot2 [22], pheatmap [23], clusterProfiler [24], and pathview [25].

Protein–Protein Molecular Docking

NEFL, NEN1, and caspase-3 predicted structures were generated by Alphafold. To ensure the accuracy of the docking results, we subsequently used AutoDockTools-1.5.7 to manually perform dehydrogenation, hydrogenation, and other optimization operations on the protein structures [26]. Protein–protein docking was then performed using the docking server (GRAMM) [27, 28]. Then the obtained protein–protein complexes were also manually subjected to optimization operations like de-watering, hydrogenation etc. using AutoDockTools-1.5.7. Finally, protein interaction prediction was performed using Pymol and protein–protein interaction maps were generated. In PyMol, NEFL was represented as a dark blue cartoon model, NEN1 was shown as a cyan cartoon model, caspase-3 was shown as a green cartoon model, and their binding sites were shown as stick structures with corresponding colors. When focusing on the binding region, the binding site is then shown with a demonstration of the protein to which it belongs.

In Vitro Experiment

Cell Culture and Infection

PC12 cells are gratefully acknowledged as a gift from Dr. Liping Su. PC12 cells were cultured in DMEM medium (Gbico), which includes 10% fetal bovine serum (FBS) (BI). All cells were cultured at 37 °C in an incubator with 5% CO_2 gas atmosphere.

Two NEFL overexpression sequence and NEFL silencing sequence lentiviruses (Shanghai Genechem Co., Ltd.) were constructed by adding the corresponding volume of lentivirus according to MOI = 10, co-culturing for 16 h, and then switching to a complete medium with puromycin added for culture and screening until the construction of stably transfected NEFL overexpression and silencing cell lines. In order to construct the model of neuronal apoptosis caused by diacetylmorphine, cells were treated with different concentrations of diacetylmorphine for 12 h; in order to detect cell viability, cells were treated with 400-μg/l diacetylmorphine for 12 h.

Fluorescence Detection

CCK-8

Cells were inoculated into 96-well plates, laid out according to 5×10^3 cells per well, and after different conditions (100 –1000 μg/l gradient diacetylmorphine intervention for 12 h; 400-μg/l diacetylmorphine intervention for 12 h) were intervened. The appropriate amount of CCK-8 reagent (Proteintech) was added. The cell viability was determined by the absorbance at 450 nm using an enzyme meter according to the instructions of the reagent.

Transmission Electron Microscope

Cells: The medium was discarded in a large petri dish, and the electron microscopy fixative was added directly, and the cells were gently scraped with a cell scraper and collected into a centrifuge tube. Then centrifuge at 1000 rpm for 3 min, discard the supernatant, add new electron microscope fixative, and fix for 2 h at room temperature. Images were obtained from Servicebio (Wuhan, China).

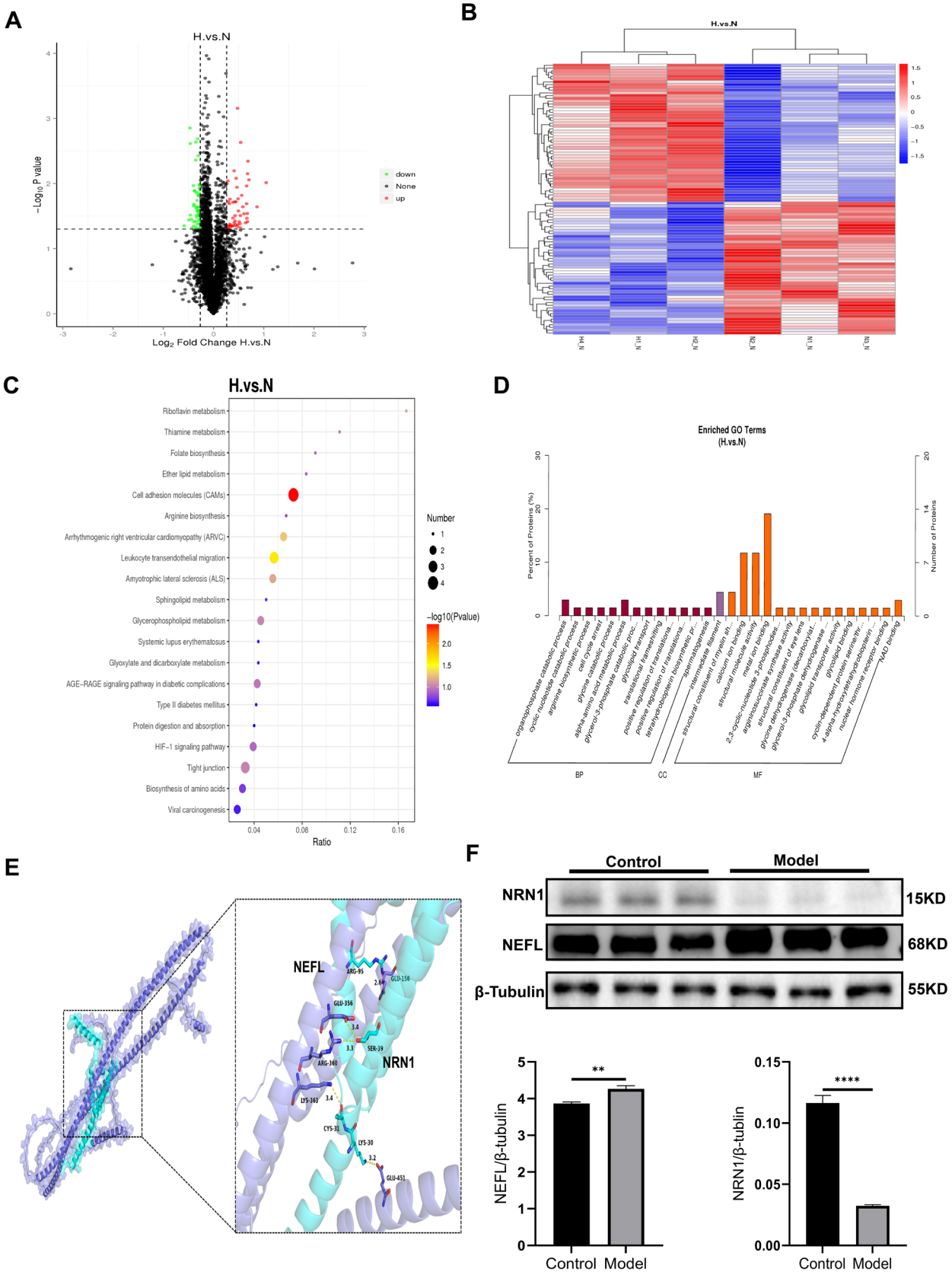
A
H.vs.N
−Log10 P value
Log2 Fold Change H.vs.N
down
None
up
B
H.vs.N
C
H.vs.N
Riboflavin metabolism
Thiamine metabolism
Folate biosynthesis
Ether lipid metabolism
Cell adhesion molecules (CAMs)
Arginine biosynthesis
Arrhythmogenic right ventricular cardiomyopathy (ARVC)
Leukocyte transendothelial migration
Amyotrophic lateral sclerosis (ALS)
Sphingolipid metabolism
Glycerophospholipid metabolism
Systemic lupus erythematosus
Glyoxylate and dicarboxylate metabolism
AGE−RAGE signaling pathway in diabetic complications
Type II diabetes mellitus
Protein digestion and absorption
HIF−1 signaling pathway
Tight junction
Biosynthesis of amino acids
Viral carcinogenesis
Ratio
Number
−log10(Pvalue)
D
Enriched GO Terms
(H.vs.N)
Percent of Proteins (%)
Number of Proteins
BP
CC
MF
E
NEFL
NRN1
F
Control
Model
NRN1
NEFL
β-Tubulin
15KD
68KD
55KD
NEFL/β-tubulin
NRN1/β-tublin
Control Model
Control Model

◂**Fig. 2** Differential gene screening and enrichment analysis of addicted rat brain tissue. **A**, **B** When FC ≥ 1.2, meanwhile *P* value ≤ 0.05, a total of 50 up-regulated expressed eggs were screened, and when FC ≤ 0.83, meanwhile *P* value ≤ 0.05, a total of 48 down-regulated expressed proteins were screened; **C**, **D** KEGG and GO enrichment of up-regulated and down-regulated genes; **E** Using the pymoland other software for molecular docking of NEFL and NRN1, dark blue model for NEFL and cyan model for NRN1; **F** Western blot to detect the protein expression levels of NEFL and NRN1, compared with control, **P* < 0.1, ***P* < 0.01, ****P* < 0.001

Cellular Mitochondrial Protein Extraction

Follow the instructions of Mitochondrial Extraction Kit (C3601), specifically, collect the more 1×10^7 cells precipitate after resuspension with pre-cooled PBS, centrifugation (600 g, 5 min) to take the precipitate and add 1 ml of a mixture of mitochondrial isolation reagent and PMSF, gently resuspension and ice bath for 15 min, homogenization, centrifugation (4 °C, 600 g, 10 min) to take the supernatant, and then centrifugation (4 °C, 11,000 g, 10 min), supernatant that is the mitochondrial proteins, and quantified and can be used for the subsequent experiments.

Flow Cytometry and Fluorescence

Apoptosis: Cells were treated with diacetylmorphine (400 μg/l) for 12 h, and apoptosis was detected by PE Annexin V Apoptosis Detection Kit I. Specifically, 100 μl of 1 × binding buffer was added with 5 μl of PE and 5 μl of annexin V. The working solution was added to the collected and washed 1 × 105 cell precipitates, incubated for 15 min at room temperature, protected from light, and then added with 400 μl of 1 × binding buffer to make a single-cell suspension for the assay.

ROS: Flow cytometry: Cells were treated with diacetylmorphine (400 μg/l) for 12 h, and total cellular ROS were detected by ROS Detection Kit (Solarbio). Specifically, 1 μl of DCFH-DA was added to 1 ml of serum-free medium to form a staining working solution. Resuspension was carried out by adding 1 ml of staining working solution for every 1 × 106 cell precipitate, and the excess staining working solution was washed out with serum-free medium after incubation for 20 min at 37 °C in a temperature chamber. Single cell suspension was made with 500 μl of serum-free medium for flow cytometry. Fluorescence: Cells were treated with diacetylmorphine (400 μg/l) for 12 h, and total cellular ROS were detected by ROS assay kit (Solarbio). The specific staining working solution is configured in the same way as described above. One milliliter of staining working solution was added to each well of a six-well plate, and incubated at 37 °C for 20 min in a cell culture incubator. Wash three times with serum-free medium to remove excess staining solution, and visualized using fluorescence inverted microscope (Nikon).

JC-1: Flow cytometry: Cells were treated with diacetylmorphine (400 μg/l) for 12 h, and cellular mitochondrial membrane potential was detected by the Jc-1 assay kit (Solarbio). Specifically, JC-1 staining working solution was configured according to JC-1 (200 ×): ultrapure water: JC-1 staining buffer (5 ×) = 5:800:200. Add 500 μl of staining working solution to each 1 × 106 cells and mix well, and incubate for 20 min at 37 °C in a temperature chamber. After washing out the excess staining solution with JC-1 staining buffer (1 ×), 500 μl of JC-1 staining buffer (1 ×) was added to prepare a single-cell suspension, which was detected by flow cytometry. Fluorescence: Cells were treated with diacetylmorphine (400 μg/l) for 12 h, and cellular mitochondrial membrane potential was detected by JC-1 assay kit (Solarbio). After the staining, working solution was configured according to the above method, 1 ml/well of staining working solution was added to the corresponding six-well plate and incubated for 20 min at 37 °C in a cell culture incubator. Use JC-1 staining buffer (1 ×) to wash out the excess staining solution and observe under fluorescence microscope.

Results

Diacetylmorphine Causes Neuronal Apoptosis

In order to investigate the specific mechanism of neuronal damage by diacetylmorphine, we firstly made a preliminary observation of the pathological and morphological changes of the brain tissue using HE staining and found that, compared with the control group, the brain tissue of the model group showed severe vacuole-like degeneration and inflammatory exudation (Fig. 1A). It suggests that the neurons in our brain tissue were severely damaged. The results of Nissl staining were similarly suggestive: compared with the control group, there was a significant decrease in Nissl bodies and a significant decrease in the number of neurons in the model group (Fig. 1B). For further verification, we took paraffin sections of brain tissues from the same area for Hoechst33342 and Tunel staining, and the results suggested that the number of apoptotic neurons in the model group was significantly increased compared with that in the control group (Fig. 1C, D). The results of Western blot showed that the number of apoptotic neurons in the damaged tissues of the model group was significantly increased compared with that in the control group. Caspase-3, caspase-9, and Bax expression were significantly upregulated, and Bcl-2 expression was significantly downregulated in the damaged brain tissues of the control group compared with the model group (Fig. 1E and F), and the results were statistically different ($P < 0.05$).

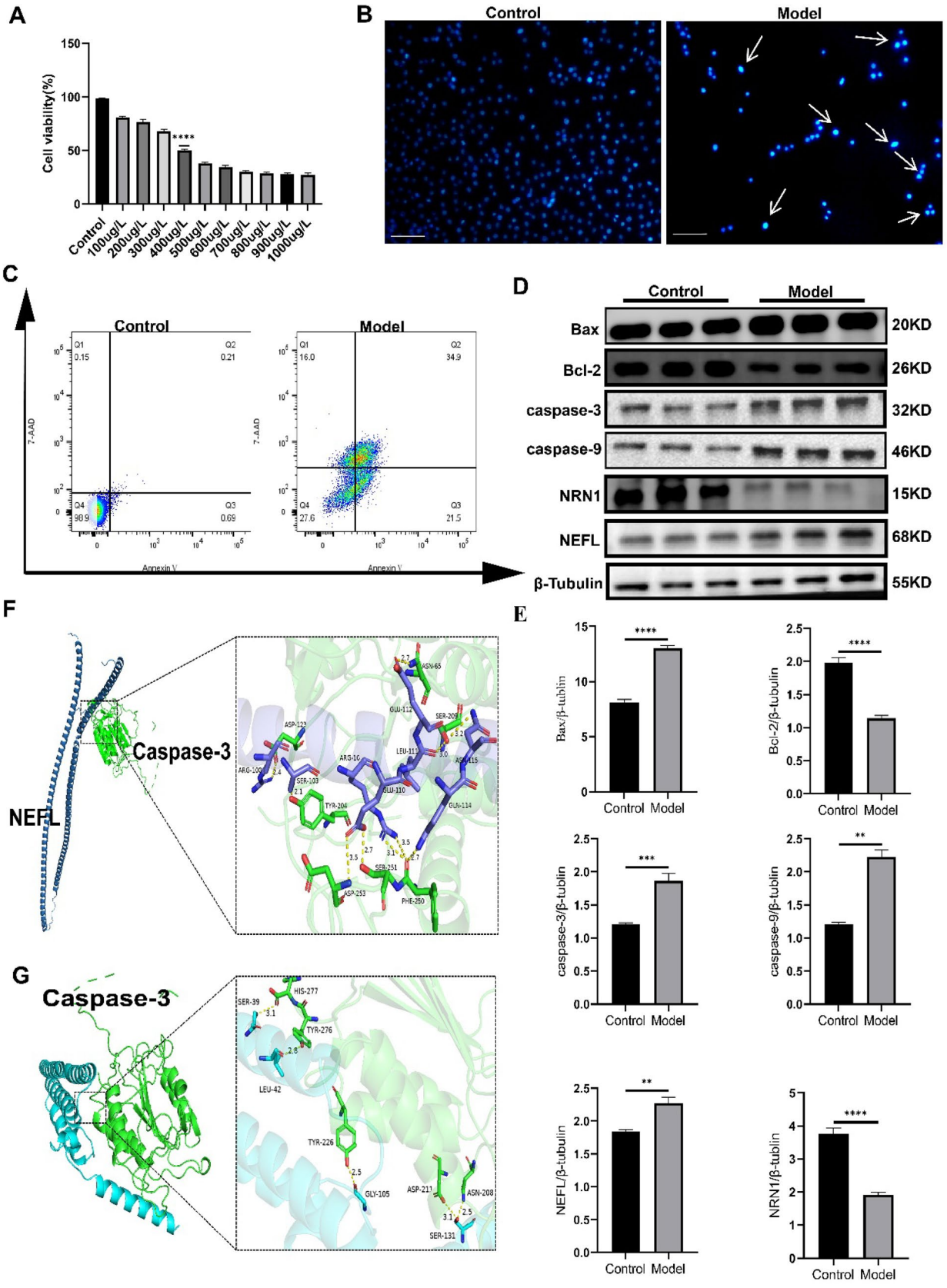
A
Cell viability(%)
150
100
50
0
****
Control
100ug/L
200ug/L
300ug/L
400ug/L
500ug/L
600ug/L
700ug/L
800ug/L
900ug/L
1000ug/L
B
Control
Model
C
Control
Model
7-AAD
Annexin V
Q1 0.15
Q2 0.21
Q4 90.9
Q3 0.69
Q1 16.0
Q2 34.9
Q4 27.6
Q3 21.5
D
Control
Model
Bax
Bcl-2
caspase-3
caspase-9
NRN1
NEFL
β-Tubulin
20KD
26KD
32KD
46KD
15KD
68KD
55KD
E
Bax/β-tubulin
Bcl-2/β-tubulin
caspase-3/β-tubulin
caspase-9/β-tubulin
NEFL/β-tubulin
NRN1/β-tubulin
Control
Model
F
Caspase-3
NEFL
G
Caspase-3

◂**Fig. 3** NEFL and NRN1 play important roles in diacetylmorphine-induced neuronal apoptosis. **A** CCK-8 to detect cell viability; **B**, **C** Hoechst33342 and flow cytometry to detect the number of apoptotic cells and apoptosis rate; **D** Western blot to detect the protein expression levels of NEFL, NRN1, caspase-3, caspase-9, Bax, Bcl-2 protein expression levels; **F**, **G** prediction of mutual binding sites between NEFL, NRN1 and caspase-3, dark blue model for NEFL, cyan model for NRN1, and green model for caspase-3; compared with control, $*P<0.1$, $**P<0.01$, $***P<0.001$

TMT Proteomics Screening for Differential Proteins

Based on the analysis of TMT proteomics data, a total of 320 differential proteins were found in diacetylmorphine-addicted rat brain tissues compared with normal rat brain tissues, with NEFL ranking among the top 10 upregulated proteins, and NRN1 among the top 10 downregulated proteins (Fig. 2A and B), and both of them were closely related to neurological disorders [29, 30], and programmed cell death [31], which aroused our great interest. To further understand the potential functions of the differential genes and the related pathways involved, we subjected all differential genes to GO and KEGG enrichment analysis. As shown (Fig. 2C, D) KEGG and GO enrichment put metabolic pathways and metabolic processes in the main position. Based on these analyses and recent studies, we found that NEFL and NRN1 function in close relation to the function and state of mitochondria, specifically mediating the close correlation between mitochondrial function and mitochondrial damage [13, 32]. In order to investigate whether there might be a correlative interaction between NEFL and NRN1, we also used protein–protein molecular docking technique to dock the molecular conformations of NEFL and NRN1, and the results showed that in the hydrogen bonding interactions, there are multiple sets of residues used to form hydrogen bonds between NEFL and NEN1, such as GLU356 of NEFL and SER39 of NEN1, i.e., there was an interaction between NEFL and NRN1 (Fig. 2E). Meanwhile, Western blot results also showed that NEFL expression was upregulated and NRN1 expression was downregulated compared with the control group, and the results were statistically significant ($P<0.05$) (Fig. 2F).

NEFL, NRN1 are Involved in Diacetylmorphine-Induced Neuronal Apoptosis

In order to further explore the specific mechanism of NEFL, NRN1 in diacetylmorphine-induced neuronal apoptosis, we firstly determined the optimal diacetylmorphine intervention condition, i.e., 400 μg/l, 12 h, using PC12 (Fig. 3A). In order to verify the correctness, we firstly stained the cells using Hoechst33342 reagent, which showed that the number of apoptotic cells in the model group was significantly increased compared with that in the control group (Fig. 3B), and secondly, the results of the apoptosis detection by flow cytometry also showed that the apoptosis rate in the model group was significantly higher than that in the control group (Fig. 3C). The expression of caspase-3 and caspase-9 in the apoptosis executing protein caspase family was detected using Western blot, and it was found that: the expression of caspase-3 and caspase-9 in the model group was much higher than that in the control group, with statistically significant differences in the results ($P<0.05$) (Fig. 3D, E). Meanwhile, compared with the control group, the protein expression of NEFL was significantly higher and that of NRN1 was significantly lower in the Model group (Fig. 3D, E). In order to further determine that NEFL and NRN1 play important roles in diacetylmorphine-induced neuronal apoptosis, we have used protein–protein molecular docking technique and found that both NEFL and NRN1 have mutual binding sites with caspase-3 (Fig. 3F, G). In summary, we concluded that NEFL, NRN1 play an important role in diacetylmorphine-induced neuronal apoptosis.

NEFL-Regulated NRN1 Acts on Neuronal Apoptosis Induced by Diacetylmorphine

To investigate whether NEFL plays a role in diacetylmorphine-induced neuronal apoptosis by regulating NRN1, we overexpressed and silenced NEFL in PC12 cells and verified the transfection efficiency using Western blot (Fig. 4A). The cell viability of control, model, oe-NEFL + M (overexpression of NEFL and intervention with diacetylmorphine), and sh-NEFL + M (silencing of NEFL and intervention with diacetylmorphine) groups was measured by CCK-8. NEFL + M groups all showed a decrease in cell viability; compared with the control group, cell viability in the oe-NEFL + M group further decreased, while cell viability in the sh-NEFL + M group increased, and all of these results were statistically different ($P<0.05$) (Fig. 4B). At the same time, we used Hoechst33342 and flow cytometry to stain apoptotic cells and detect the apoptosis rate, and the results showed that the number of apoptotic cells as well as the apoptosis rate increased in the model, oe-NEFL + M, and sh-NEFL + M groups compared with the control group; the number of apoptotic cells as well as the apoptosis rate further increased in the oe-NEFL + M group compared with the model group; the number of apoptotic cells as well as the apoptosis rate further increased in the model group compared with the model group; the number of apoptotic cells as well as the apoptosis rate further increased in the sh-NEFL + M group. The number of apoptotic cells and the apoptotic rate were further increased in the oe-NEFL + M group, while the number of apoptotic cells and the apoptotic rate were decreased in the sh-NEFL + M group (Fig. 4C, D). At the molecular level, compared with the control group, the apoptosis-related factors caspase-3, caspase-9, and Bax protein expression

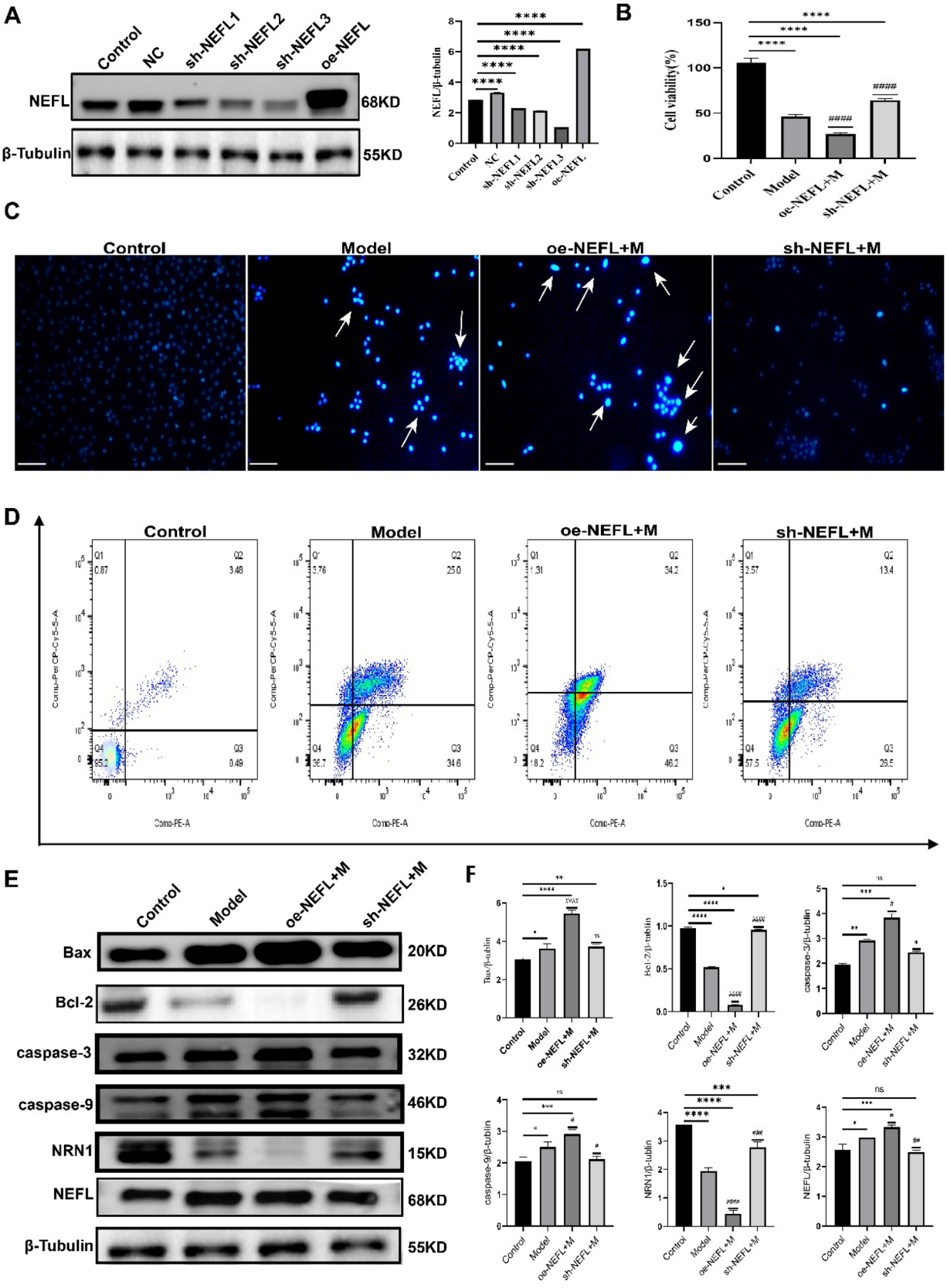
A
Control
NC
sh-NEFL1
sh-NEFL2
sh-NEFL3
oe-NEFL
NEFL
68KD
β-Tubulin
55KD
NEFL/β-tubulin
B
Cell viability(%)
Control
Model
oe-NEFL+M
sh-NEFL+M
C
Control
Model
oe-NEFL+M
sh-NEFL+M
D
Control
Model
oe-NEFL+M
sh-NEFL+M
Comp-PerCP-Cy5-5-A
Comp-PE-A
Q1
Q2
Q3
Q4
0.87
3.48
0.49
95.2
3.76
25.0
34.6
36.7
1.31
34.2
46.2
18.2
2.57
13.4
28.5
57.5
E
Control
Model
oe-NEFL+M
sh-NEFL+M
Bax
20KD
Bcl-2
26KD
caspase-3
32KD
caspase-9
46KD
NRN1
15KD
NEFL
68KD
β-Tubulin
55KD
F
Bax/β-tubulin
Bcl-2/β-tubulin
caspase-3/β-tubulin
caspase-9/β-tubulin
NRN1/β-tubulin
NEFL/β-tubulin

◂**Fig. 4** NEFL can affect NRN1 expression and neuronal apoptosis. **A** NEFL transfection efficiency; **B** CCK-8 to detect cell viability; **C**, **D** Hoechst33342 and flow cytometry to detect the number of apoptotic cells and the rate of apoptosis; **E** Western blot to detect the NEFL, NRN1, caspase-3, caspase-9, Bax, and Bcl-2 protein expression levels; **F** statistics for E; compared with control, $^{*}P<0.1$, $^{**}P<0.01$, $^{***}P<0.001$, $^{****}P<0.0001$; compared with model, $^{\#}P<0.1$, $^{\#\#}P<0.01$, $^{\#\#\#}P<0.001$, $^{\#\#\#\#}P<0.0001$

were increased and Bcl-2 protein expression was decreased in the model and oe-NEFL + M groups, and caspase-3, caspase-9, Bax, and Bcl-2 protein expression was decreased in the sh-NEFL + M group. expression was in contrast to the model group, oe-NEFL + M. When compared with the model group, the expression of caspase-3, caspase-9, and Bax proteins was increased and the expression of Bcl-2 protein was decreased in the oe-NEFL + M group, and the opposite was observed in the sh-NEFL + M group, and the results were all statistically different ($P<0.05$) (Fig. 4E, F).

NEFL Regulates NRN1-Mediated Mitochondrial Pathway Action

In order to further investigate whether diacetylmorphine-induced neuronal apoptosis is caused by the mitochondrial pathway, we firstly used transmission electron microscopy to observe the ultrastructural alterations of the cells in control and model groups, and found that compared with the control group, the morphology of mitochondria in the model group was highly impaired, presenting dilated, vacuole-like alterations, one of the alterations of mitochondria in the apoptotic cells [33] (Fig. 5A). Secondly, we detected intracellular ROS accumulation and mitochondrial membrane potential changes to further confirm the cause of mitochondrial morphology and functional disruption, and the results showed that, compared with the control group, intracellular ROS accumulation was increased and mitochondrial membrane potential was decreased in the model, oe-NEFL + M, and sh-NEFL + M groups, and, compared with the model group, the oe-NEFL + M group showed an increase in intracellular ROS accumulation and a decrease in mitochondrial membrane potential, and, compared with the model group, the oe-NEFL + M group showed a decrease in intracellular ROS accumulation. NEFL + M group showed a further increase in intracellular ROS accumulation and a more significant decrease in mitochondrial membrane potential, while the sh-NEFL + M group showed a significant decrease in intracellular ROS content and an increase in mitochondrial membrane potential, which tended to be normal (Fig. 5B, C, D, and E). Western blot detection of cytochrome c in the cytoplasm and mitochondria revealed that, compared with the control group, cytochrome c protein expression was increased in the cytoplasm and decreased in the mitochondria in the model, oe-NEFL + M, and sh-NEFL + M groups, compared with the control group; cytochrome c protein expression was elevated in the cytoplasm in the oe-NEFL + M group, decreased in the mitochondria, and opposite in the mitochondria, compared with the control group; cytochrome c protein expression was increased in the model group, and decreased in the mitochondria, and opposite in the mitochondria, compared with the control group. decreased in mitochondria, and the opposite in mitochondria, and the results were all statistically different ($P<0.05$) (Fig. 5F,G).

Discussions

Diacetylmorphine is the most abused of the opioids, with 31.5 million deaths per year globally caused by overdose or injection. Due to its strong euphoric, addictive, and neurotoxic properties, most of the "chasing the dragon" patients often suffer severe neurological damage, showing clinical symptoms such as mania, schizophrenia, and cerebellar ataxia [34].Unfortunately, reports on the mechanisms of their associated disease development have still not been identified. In the current study, we demonstrated that NEFL, NRN1 play an important role in diacetylmorphine-induced neuronal apoptosis. Mechanistically, NEFL further mediates the mitochondrial pathway in diacetylmorphine-induced neuronal apoptosis through the regulation of NRN1.

NEFL plays an important role in several neurodegenerative diseases and is involved in the regulation of programmed cell death. For example, a 14.1-year long follow-up in 52,645 normal people found that NEFL was consistently and strongly associated with Alzheimer's disease (AD) [29]. High expression of NEFL promotes the development of MPTP-induced Parkinson's disease (PD) in zebrafish [35]. The results showed that NEFL expression was higher in the brain tissue of diacetylmorphine-addicted rats. Similarly, in the cellular model of diacetylmorphine-induced apoptosis, the expression of NEFL was increased in the model group compared to the control group. The high expression of NEFL had a lower survival rate in the model. This also validates the result that NEFL is specifically highly expressed in the TMT proteomics of damaged brain tissue in diacetylmorphine-addicted rats. In addition, low expression of NEFL reduces the occurrence of apoptosis in the model, suggesting that NEFL promotes diacetylmorphine-induced neuronal apoptosis.

Mitochondrial pathway is one of the important pathways of apoptosis, which plays a crucial role in the regulation of endogenous apoptosis [36, 37]. NRN1 is a small, highly conserved extracellular membrane protein that plays an important role in neurological disorders [13]. Elevated expression of NRN1 inhibits the mitochondrial pathway, thereby attenuating apoptosis in retinal ganglion cells [30]. It has been shown that apoptosis of microglia promotes the development

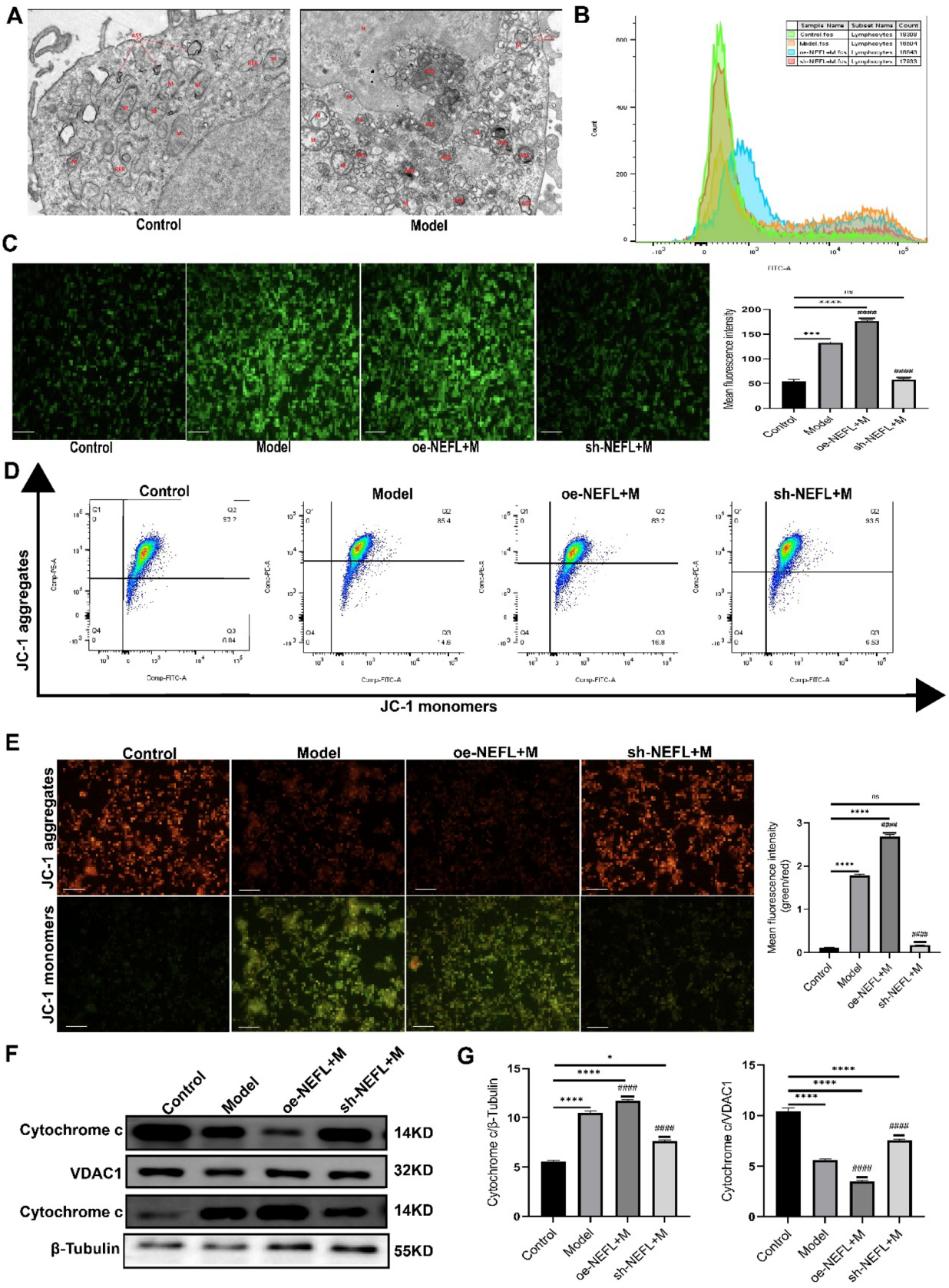
A
Control
Model
B
Sample Name
Subset Name
Count
Control.fcs
Lymphocytes
Model.fcs
Lymphocytes
oe-NEFL+M.fcs
Lymphocytes
sh-NEFL+M.fcs
Lymphocytes
Count
FITC-A
C
Control
Model
oe-NEFL+M
sh-NEFL+M
Mean fluorescence intensity
D
Control
Model
oe-NEFL+M
sh-NEFL+M
JC-1 aggregates
JC-1 monomers
E
Control
Model
oe-NEFL+M
sh-NEFL+M
JC-1 aggregates
JC-1 monomers
Mean fluorescence intensity (green/red)
F
Control
Model
oe-NEFL+M
sh-NEFL+M
Cytochrome c
VDAC1
Cytochrome c
β-Tubulin
14KD
32KD
14KD
55KD
G
Cytochrome c/β-Tubulin
Cytochrome c/VDAC1

◂**Fig. 5** NEFL can modulate NRN1 and mitochondrial pathway to affect neuronal apoptosis. **A** TEM observation of mitochondrial morphology, M indicates mitochondria in the figure; **B**, **C** intracellular ROS flow cytometry and fluorescence detection; **D**, **E** mitochondrial membrane potential flow cytometry and fluorescence detection; **F** Western blot detection of cytoplasmic and mitochondrial cytochrome c protein expression changes; **G** statistics for F; compared with control; compared with model, $^{*}P<0.1$, $^{**}P<0.01$, $^{***}P<0.001$; $^{\#}P<0.1$, $^{\#\#}P<0.01$, $^{\#\#\#}P<0.001$, $^{\#\#\#\#}P<0.0001$

of spongy white matter encephalopathy caused by the use of diacetylmorphine that elevated mitochondrial pathway-associated Bax protein expression can be detected, and that coenzyme Q10 supplementation attenuates the progression of the disease [34, 38]. Our results suggest that there is a mutual binding site and possible interaction between NRN1 and caspase-3. Caspase family, as the transmitter and effector of apoptotic priming, will turn on the intracellular death program when activated by external stimuli or regulation, further hydrolyze the downstream caspase family proteins through heterologous activation, and amplify apoptotic signals in a cascade that ultimately leading to cell death [39]. Our results identified the involvement of NRN1 in diacetylmorphine-induced neuronal apoptosis; after silencing NEFL and diacetylmorphine intervention, NRN1 expression was elevated and apoptosis levels decreased. Our results suggest that NEFL modulation of NRN1 affects diacetylmorphine-induced apoptosis.

When mitochondrial pathway plays an important role in apoptosis, mitochondrial morphology and structure are often seriously damaged, and mitochondrial membrane potential significantly decreases. Studies have shown that ROS accumulation may be the "culprit" of all this [40, 41]. Studying the roles played by mitochondria and mitochondrial pathways in apoptosis and exploring the possible regulatory mechanisms have become an important focus of target development studies for related neurological diseases. Although, the development of related drugs has achieved considerable results, it still fails to alleviate the quality of survival of patients with diacetylmorphine-induced neurological disorders.

In our study, we found that the mitochondrial pathway was activated in the diacetylmorphine model of neuronal apoptosis, as evidenced by the severe disruption of mitochondrial morphology, the presence of large numbers of vacuoles and dilated mitochondria, a significant decrease in mitochondrial membrane potential, and a severe accumulation of ROS. At the molecular level, aberrant expression of several proteins also indicates activation of the mitochondrial pathway in apoptosis. In the mitochondrial pathway, Bax receives apoptotic signals and constitutes a transmembrane channel on the mitochondrial surface, leading to a decrease in membrane potential and an increase in membrane permeability, resulting in the release of apoptotic factors; cytochrome C is released into the cytoplasm due to an increase in the permeability of the mitochondrial membrane, leading to further disruption of the mitochondrial electron transport chain, and ultimately leading to apoptosis [42, 43]. In our experiments, similarly elevated protein expression of cytochrome C in Bax and cytoplasm and decreased cytochrome C protein expression in mitochondria were found in the model group. In addition, the accumulation of ROS, the decrease in mitochondrial membrane potential, and the increase in cytoplasmic cytochrome C were ameliorated after silencing NEFL, suggesting that NEFL can mediate the mitochondrial pathway to influence diacetylmorphine-induced neuronal apoptosis.

Several studies have reported the role of NRN1 in neuroapoptosis and its close association with the mitochondrial pathway [44, 45]. Meanwhile, the mitochondrial pathway is one of the most classical signaling pathways in apoptosis [46]. Based on these studies, it is reasonable to infer that NRN1 plays an important role in diacetylmorphine-induced apoptosis and mediates the mitochondrial pathway, and the experimental results also indicate that NRN1 is involved in diacetylmorphine-induced apoptosis in neurons and is closely related to the mitochondrial pathway. Unfortunately, we have not been able to provide stronger evidence to demonstrate the specific mechanism by which NRN1 regulates the mitochondrial pathway.

In conclusion, NEFL exacerbates diacetylmorphine-induced neuronal apoptosis by modulating the NRN1-mediated mitochondrial pathway, thereby accelerating the accumulation of ROS, the decrease in mitochondrial membrane potential, and the release of cytochrome C. NEFL may serve as a new target for the treatment of neurological disorders caused by diacetylmorphine. Of course, it has to be recognized that ours still has some variability in the use of rats to construct a diacetylmorphine addiction model compared to the real human in vivo. Moreover, our study has not yet clarified the downstream targets that NRN1 interacts with and participates in apoptosis, and what factors increase the protein expression level of NEFL. However, our study still strongly suggests a possible mechanism by which diacetylmorphine abuse contributes to the onset of neuronal apoptosis that has not yet been clarified, and provides two promising therapeutic targets.

Author Contribution Ss Z designed the study and wrote the main manuscript. Ss Z performed the experiments and analyzed the data. Hw P, Lp S, and L Y revised the manuscript. Mj Z and L L prepared Figs. 1–2. M J and Lj L prepared Figs. 3–4. Jl X and Yl G prepared Figs. 3–4. Hw P supervised the study. All authors reviewed and approved the final manuscript.

Funding This work was supported by the National Natural Science Foundation of China (Grant numbers [82360256], [82160055], and [82460257]).

Data Availability No datasets were generated or analysed during the current study.

Declarations

Ethical Approval All animal experiments were approved by the Medical Ethics Committee for Animal Experiments of the First Affiliated Hospital of Xinjiang Medical University (A230307-48).

Consent for Publication We obtained permissions from the participants to publish their data. All participants gave written consent for publication.

Competing Interests The authors declare no competing interests.

References

1. Milella MS, D'Ottavio G, De Pirro S et al (2023) Heroin and its metabolites: relevance to heroin use disorder. Transl Psychiatry 13(1):120. https://doi.org/10.1038/s41398-023-02406-5
2. World Drug Report 2023 https://news.un.org/zh/story/2023/06/1119162
3. Lee JJ, Saraiya N, Kuzniewicz MW (2023) Prenatal opioid exposure and neurodevelopmental outcomes. J Neurosurg Anesthesiol 35(1):142–146. https://doi.org/10.1097/ANA.0000000000000876
4. Halloran O, Ifthikharuddin S, Samkoff L (2005) Leukoencephalopathy from "chasing the dragon." Neurology 64(10):1755. https://doi.org/10.1212/01.WNL.0000149907.63410.DA
5. O'Rourke MG, Ellem KA (2000) John Kerr and apoptosis. Med J Aust 173(11–12):616–617. https://doi.org/10.5694/j.1326-5377.2000.tb139362.x
6. Li L, Song JJ, Zhang MX et al (2023) Oridonin ameliorates caspase-9-mediated brain neuronal apoptosis in mouse with ischemic stroke by inhibiting RIPK3-mediated mitophagy. Acta Pharmacol Sin 44(4):726–740. https://doi.org/10.1038/s41401-022-00995-3
7. Schmitt R, Qayum S, Pliss A et al (2023) Mitochondrial dysfunction and apoptosis in brain microvascular endothelial cells following blast traumatic brain injury. Cell Mol Neurobiol 43(7):3639–3651. https://doi.org/10.1007/s10571-023-01372-2
8. Li S, Xiao J, Huang C, Sun J (2023) Identification and validation of oxidative stress and immune-related hub genes in Alzheimer's disease through bioinformatics analysis. Sci Rep 13(1):657. https://doi.org/10.1038/s41598-023-27977-7
9. Huang Z, Zhuo Y, Shen Z et al (2014) The role of NEFL in cell growth and invasion in head and neck squamous cell carcinoma cell lines. J Oral Pathol Med 43(3):191–198. https://doi.org/10.1111/jop.12109
10. Nedivi E, Hevroni D, Naot D et al (1993) Numerous candidate plasticity-related genes revealed by differential cDNA cloning. Nature 363:718–722. https://doi.org/10.1038/363718a0
11. Almodóvar-Payá C, Guardiola-Ripoll M, Giralt-López M et al (2022) NRN1 gene as a potential marker of early-onset schizophrenia: evidence from genetic and neuroimaging approaches. Int J Mol Sci 23(13):7456. https://doi.org/10.3390/ijms23137456. (**Published 2022 Jul 5**)
12. Du W, Gao A, Herman JG et al (2021) Methylation of NRN1 is a novel synthetic lethal marker of PI3K-Akt-mTOR and ATR inhibitors in esophageal cancer. Cancer Sci 112(7):2870–2883. https://doi.org/10.1111/cas.14917
13. Huang T, Li H, Zhang S et al (2021) Nrn1 overexpression attenuates retinal ganglion cell apoptosis, promotes axonal regeneration, and improves visual function following optic nerve crush in rats. J Mol Neurosci 71(1):66–79. https://doi.org/10.1007/s12031-020-01627-3
14. Harrington JS, Ryter SW, Plataki M et al (2023) Mitochondria in health, disease, and aging. Physiol Rev 103(4):2349–2422. https://doi.org/10.1152/physrev.00058.2021
15. Victorelli S, Salmonowicz H, Chapman J et al (2023) Apoptotic stress causes mtDNA release during senescence and drives the SASP. Nature 622(7983):627–636. https://doi.org/10.1038/s41586-023-06621-4
16. Kommalapati VK, Kumar D, Tangutur AD (2020) Inhibition of JNJ-26481585-mediated autophagy induces apoptosis via ROS activation and mitochondrial membrane potential disruption in neuroblastoma cells. Mol Cell Biochem 468(1–2):21–34. https://doi.org/10.1007/s11010-020-03708-8
17. Yang S, Liu Y, Guo Y et al (2020) Circadian gene Clock participates in mitochondrial apoptosis pathways by regulating mitochondrial membrane potential, mitochondria out membrane permeablization and apoptosis factors in AML12 hepatocytes. Mol Cell Biochem 467(1–2):65–75. https://doi.org/10.1007/s11010-020-03701-1
18. Ji M, Su L, Liu L et al (2023) CaMKII regulates the proteins TPM1 and MYOM2 and promotes diacetylmorphine-induced abnormal cardiac rhythms. Sci Rep 13(1):5827. https://doi.org/10.1038/s41598-023-32941-6. (**Published 2023 Apr 10**)
19. R Core Team (year). R: a language and environment for statistical computing. R Foundation for Statistical Computing, Vienna, Austria. URL https://www.R-project.org/
20. Wickham H, François R, Henry L, Müller K, Vaughan D (2023) _dplyr: a grammar of data manipulation_. Rpackage version 1.1.4
21. Wickham H, Averick M, Bryan J, Chang W, McGowan LD, François R, Grolemund G, Hayes A, Henry L, Hester J, Kuhn M, Pedersen TL, Miller E, Bache SM, Müller K, Ooms J, Robinson D, Seidel DP, Spinu V, Takahashi K, Vaughan D, Wilke C, Woo K, Yutani H (2019) Welcome to the tidyverse. J Open Source Softw 4(43):1686. https://doi.org/10.21105/joss.01686
22. Wickham H (2016) ggplot2: elegant graphics for data analysis. Springer-Verlag, New York
23. Kolde R (2019) _pheatmap: Pretty Heatmaps_. R package version 1:12
24. Yu G, Wang L-G, Han Y, He Q-Y (2012) clusterProfiler: an R package for comparing biological themes among gene clusters. OMICS: J Integr Biol 16(5):284–287
25. Luo W, Brouwer C (2013) Pathview: an R/Bioconductor package for pathway-based data integration and visualization. Bioinformatics 29(14):1830–1831. https://doi.org/10.1093/bioinformatics/btt285

26 Morris GM, Huey R, Olson AJ (2008) Using AutoDock for ligand-receptor docking. Current protocols in bioinformatics. Curr Protoc Bioinforma 24:8.14.1-8.14.40. https://doi.org/10.1002/0471250953.bi0814s24

27. Katchalski-Katzir E, Shariv I, Eisenstein M et al (1992) Molecular surface recognition: determination of geometric fit between proteins and their ligands by correlation techniques. Proc Natl Acad Sci USA 89:2195–2199. https://doi.org/10.1073/pnas.89.6.2195

28. Vakser IA (1996) Long-distance potentials: an approach to the multiple-minima problem in ligand-receptor interaction. Protein Eng 9:37–41. https://doi.org/10.1093/protein/9.1.37

29. Guo Y, You J, Zhang Y et al (2024) Plasma proteomic profiles predict future dementia in healthy adults. Nat Aging 4(2):247–260. https://doi.org/10.1038/s43587-023-00565-0

30. Almodóvar-Payá C, Guardiola-Ripoll M, Giralt-López M et al (2022) NRN1 gene as a potential marker of early-onset schizophrenia: evidence from genetic and neuroimaging approaches. Int J Mol Sci 23(13):7456. https://doi.org/10.3390/ijms23137456

31. Hsiao CP, Wang D, Kaushal A et al (2013) Mitochondria-related gene expression changes are associated with fatigue in patients with nonmetastatic prostate cancer receiving external beam radiation therapy. Cancer Nurs 36(3):189–197. https://doi.org/10.1097/NCC.0b013e318263f514

32. Gentil BJ, Mushynski WE, Durham HD (2013) Heterogeneity in the properties of NEFL mutants causing Charcot-Marie-Tooth disease results in differential effects on neurofilament assembly and susceptibility to intervention by the chaperone-inducer, celastrol. Int J Biochem Cell Biol 45(7):1499–1508. https://doi.org/10.1016/j.biocel.2013.04.009

33. Feldmann G, Haouzi D, Moreau A et al (2000) Opening of the mitochondrial permeability transition pore causes matrix expansion and outer membrane rupture in Fas-mediated hepatic apoptosis in mice. Hepatology 31(3):674–683. https://doi.org/10.1002/hep.510310318

34. Kashyap S, Majeed G, Bowen I et al (2020) Toxic leukoencephalopathy due to inhalational heroin abuse. Ann Indian Acad Neurol 23(4):542–544. https://doi.org/10.4103/aian.AIAN_446_18

35. Sarath Babu N, Murthy ChL, Kakara S et al (2016) 1-Methyl-4-phenyl-1,2,3,6-tetrahydropyridine induced Parkinson's disease in zebrafish. Proteomics 16(9):1407–1420. https://doi.org/10.1002/pmic.201500291

36. Tang Q, Chen H, Mai Z et al (2022) Bim- and Bax-mediated mitochondrial pathway dominates abivertinib-induced apoptosis and ferroptosis. Free Radic Biol Med 180:198–209. https://doi.org/10.1016/j.freeradbiomed.2022.01.013

37. Zhang S, Rao S, Yang M et al (2022) Role of mitochondrial pathways in cell apoptosis during He-Patic ischemia/reperfusion injury. Int J Mol Sci 23(4):2357. https://doi.org/10.3390/ijms23042357

38. Yin RX, Lu JY, Lu BX, et al. (2020) Zhonghua Yi Xue Za Zhi. 2008;88(11):749–753

39. Van Opdenbosch N, Lamkanfi M (2019) Caspases in cell death, inflammation, and disease. Immunity 50(6):1352–1364. https://doi.org/10.1016/j.immuni.2019.05.020

40 Green DR, Reed JC (1998) Mitochondria and apoptosis. Science. 281(5381):1309–1312. https://doi.org/10.1126/science.281.5381.1309

41. Sinha K, Das J, Pal PB et al (2013) Oxidative stress: the mitochondria-dependent and mitochondria-independent pathways of apoptosis. Arch Toxicol 87(7):1157–1180. https://doi.org/10.1007/s00204-013-1034-4

42. Luna-Vargas MPA, Chipuk JE (2016) Physiological and pharmacological control of BAK, BAX, and beyond. Trends Cell Biol 26(12):906–917. https://doi.org/10.1016/j.tcb.2016.07.002

43. Lemasters JJ, Qian T, He L et al (2002) Role of mitochondrial inner membrane permeabilization in necrotic cell death, apoptosis, and autophagy. Antioxid Redox Signal 4(5):769–781. https://doi.org/10.1089/152308602760598918

44. Wang T, Cheng Y, Han H et al (2019) miR-194 accelerates apoptosis of Aβ1¯42-transduced hippocampal neurons by inhibiting Nrn1 and decreasing PI3K/Akt signaling pathway activity. Genes (Basel) 10(4):313. https://doi.org/10.3390/genes10040313

45. Zammit AR, Klein HU, Yu L et al (2024) Proteome-wide analyses identified cortical proteins associated with resilience for varied cognitive abilities. Neurology 102(1):e207816. https://doi.org/10.1212/WNL.0000000000207816

46. Green DR, Fitzgerald P (2016) Just so stories about the evolution of apoptosis. Curr Biol 26(13):R620–R627. https://doi.org/10.1016/j.cub.2016.05.023